RSC Advances

PAPER

View Article Online
View Journal | View Issue

Cite this: *RSC Adv.*, 2026, **16**, 17310

ent-Pimarane diterpenoids from the aerial parts of *Sigesbeckia pubescens* and their myocardial protective activity

Wanting Li,†[a] Guiyang Xia,†[ab] Jinyu Xia,[bc] Qiyao Liu,[b] Xuefen Wu,[b] Linnan Zhou,[a] Xiaohong Wei,[b] Huan Xia*[ab] and Sheng Lin *[ab]

Received 14th December 2025
Accepted 5th March 2026

DOI: 10.1039/d5ra09664b

rsc.li/rsc-advances

Eight new *ent*-pimarane diterpenoids (**1–8**), along with three known compounds (**9–11**), were isolated from the aerial parts of *Sigesbeckia pubescens*. The structures of the new *ent*-pimarane diterpenoids were established by extensive spectroscopic techniques, X-ray diffraction crystallography, ECD calculations and $Mo_2(OAc)_4$-induced ECD. The isolated compounds were evaluated for their myocardial protective activities in an H9c2 cell hypoxia/reoxygenation (H/R) induced myocardial ischemia-reperfusion injury model. Bioassay results showed that pubescens B (**2**), pubescens H (**8**) and darutigenol (**9**) enhanced the cell viability at concentrations of 1, 10, and 50 μM and molecular docking explored their binding mode with H/R connected protein Ubiquitin C-terminal hydrolase L5 (UCHL5).

Introduction

Herba Siegesbeckiae (HS, the aerial parts of *Sigesbeckia orientalis* L., *S. glabrescens* Makino, and *S. pubescens* Makino from the genus *Sigesbeckia* of the Asteraceae family), first recorded in *Xin Xiu Ben Cao* in the Tang dynasty, has the effects of detoxifying, clearing meridians, and dispelling wind and damp, and has been traditionally used for the therapy of rheumatoid arthritis, hypertension, snakebites, and malaria.[1] Also, *Lin Zheng Zhi Nan Yi An* mentioned that HS has been effectively applied to treat cardio-cerebrovascular diseases. For example, Xixian Tongshuan Capsule and Xinshuning Tablet with HS as the monarch herb have been listed in the Chinese Pharmacopoeia (2025 edition) for the treatment of coronary heart disease and stroke.[2,3] The pharmacological research demonstrated that the traditional use of HS for the above diseases was attributed to its anti-inflammatory,[4,5] antiallergic,[6] angiogenesis,[7] myocardial protective[8–10] and antioxidant activities.[11] Previous chemical studies showed that a total of 291 compounds have been isolated and characterized from the three *Sigesbeckia* species, including *ent*-kaurane and *ent*-pimarane diterpenoids, sesquiterpenoids, sterols, and flavonoids.[12–14] Among them, *ent*-kaurane and *ent*-pimarane diterpenoids are the primary bioactive constituents of HS.

With the development of mechanism and medication research to prevent myocardial H/R injury, increasingly preclinical evidence has supported the therapeutic effect of traditional Chinese medicine.[15–17] Our previous study has also found that UCHL5 can affect the NLRP3 inflammasome during myocardial H/R, and the fraction of HS can inhibit the UCHL5/NLRP3 pathway to alleviated myocardial H/R injury. Furthermore, a chemical and molecular docking experiment showed that an *ent*-pimarane diterpenoid, kirenol, might be the core active constituent.[18,19] In order to discover more myocardial protective compounds from HS and as part of our ongoing screening program toward new lead compound discovery from Chinese medicinal plants, further chemical investigation on the aerial parts of *S. pubescens* led to the isolation of eight new *ent*-pimarane diterpenoids (**1–8**) named pubescens A–H and three known analogues (**9–11**) (Fig. 1). We described herein the isolation and structural elucidation of **1–11**. Furthermore, all isolated compounds were tested for myocardial protective activity by H9c2 cardiomyocytes hypoxia/reoxygenation (H/R) induced myocardial ischemia-reperfusion injury model. We identified that pubescens B (**2**) and pubescens H (**8**) had good myocardial protective function, and discussed the interaction between the active compounds and UCHL5.

Results and discussion

The 95% EtOH extracts of the aerial parts of *S. pubescens* (15 kg) were systematically separated by ODS column, Sephadex LH-20, and preparative HPLC to yield compounds **1–11**.

[a]*School of Chinese Materia Medica, Beijing University of Chinese Medicine, Beijing, 102488, China*

[b]*Key Laboratory of Chinese Internal Medicine of Ministry of Education and Beijing, Dongzhimen Hospital, Beijing University of Chinese Medicine, Beijing, 100700, China. E-mail: lsznn@126.com; xiahuan@bucm.edu.cn*

[c]*Key Laboratory of Structure-Based Drug Design & Discovery, Ministry of Education, Wuya College of Innovation, Shenyang Pharmaceutical University, Shenyang, 110016, China*

† These authors contributed equally to this work.

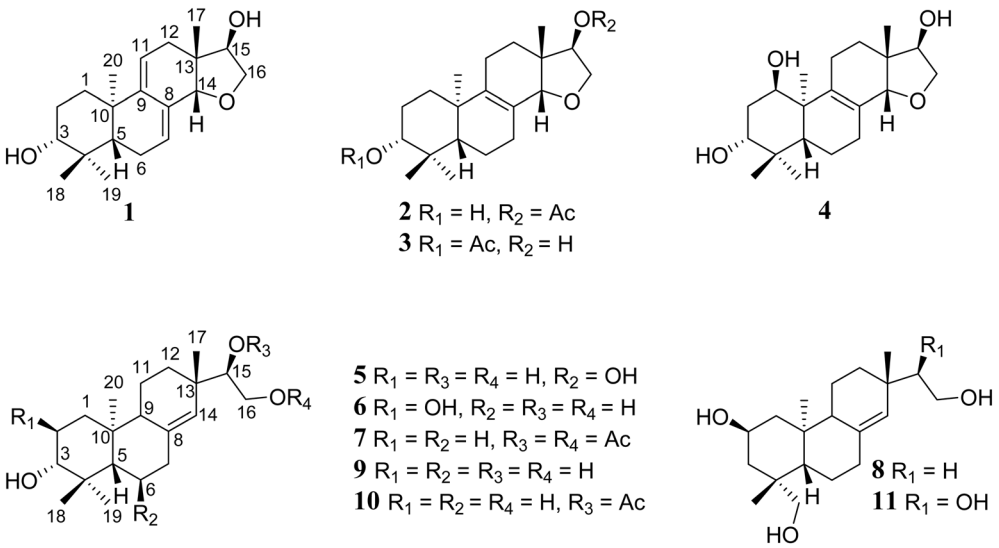

Fig. 1 Structures of compounds **1–11**.

Compound **1** was obtained as a white powder with $[\alpha]$ +52.0. Its molecular formula was determined to be $C_{20}H_{30}O_3$ by (+)-HRESIMS data at *m/z* 319.2276 $[M + H]^+$ (calcd for $C_{20}H_{31}O_3$, 319.2267), indicating 6 degrees of unsaturation. The IR analysis presented the signals of hydroxy (3387 cm^{-1}) and double-bond (1682 cm^{-1}). The ^1H NMR spectrum (Table 1) showed characteristic signals for three oxygenated methine protons [δ_H 3.16 (1H, dd, $J = 11.2$, 5.6 Hz), 3.83 (1H, dd, $J = 1.4$, 5.6 Hz), 3.90 (1H,

Table 1 ^1H and ^{13}C NMR spectroscopic data of compounds **1** and **2** in CD_3OD

	1		**2**	
Position	δ_H (J in Hz)[a]	δ_C[b], type	δ_H (J in Hz)[a]	δ_C[b], type
1a	1.88, dt (15.4, 4.2)	36.5, CH_2	1.83, dt (13.2, 3.6)	35.5, CH_2
1b	1.49, td (15.4, 4.8)		1.20 td (13.2, 5.4)	
2a	1.72 m	28.3, CH_2	1.67, m	28.2, CH_2
2b	1.70, m		1.65, m	
3	3.16, dd (11.2, 5.6)	79.6, CH	3.18, dd (10.8, 5.4)	79.5, CH
4		40.1, C		39.9, C
5	1.24, dd (11.9, 4.9)	50.0, CH	1.11, dd (12.6, 2.4)	52.0, CH
6a	2.27, dt (18.2, 4.9)	25.0, CH_2	1.77, dd (12.6, 7.2)	19.6, CH_2
6b	2.21, dd (18.2, 11.9)		1.53, ddd (18.6, 12.6, 6.0)	
7a	5.87, d (5.6)	131.9, CH	2.39, td (17.4, 5.4)	31.8, CH_2
7b			1.92, m	
8		129.6, C		125.2, C
9		144.6, C		143.1, C
10		37.6, C		38.8, C
11a	5.33, t (4.2)	115.6, CH	2.05, m	21.8, CH_2
11b			2.03, m	
12a	1.87, m	34.0, CH_2	1.46, m	29.9, CH_2
12b	1.86, m		1.35, td (12.0, 6.6)	
13		45.2, C		43.1, C
14	3.90, s	84.7, CH	3.56, s	84.5, CH
15	3.83, dd (5.6, 1.4)	79.5, CH	4.89, dd (5.4, 2.4)	82.7, CH
16a	4.30, dd (11.9, 5.6)	75.3, CH_2	4.26, dd (10.8, 5.4)	72.3, CH_2
16b	3.59, dd (11.9, 1.4)		3.62, dd (10.8, 2.4)	
17	0.92, s	16.3, CH_3	0.90, s	14.6, CH_3
18	0.98, s	28.4, CH_3	1.01, s	28.6, CH_3
19	0.89, s	16.0, CH_3	0.82, s	16.3, CH_3
20	0.98, s	21.3, CH_3	1.02, s	19.7, CH_3
OAc-15			2.08, s	172.3, C
				20.8, CH_3

[a] ^1H NMR data (d) were measured in 600 MHz NMR instrument. Proton coupling constants (J) in Hz are given in parentheses. [b] ^{13}C data were recorded at 150 MHz. The assignments were based on ^1H–^1H COSY, HSQC, HMBC, and NOESY experiments.

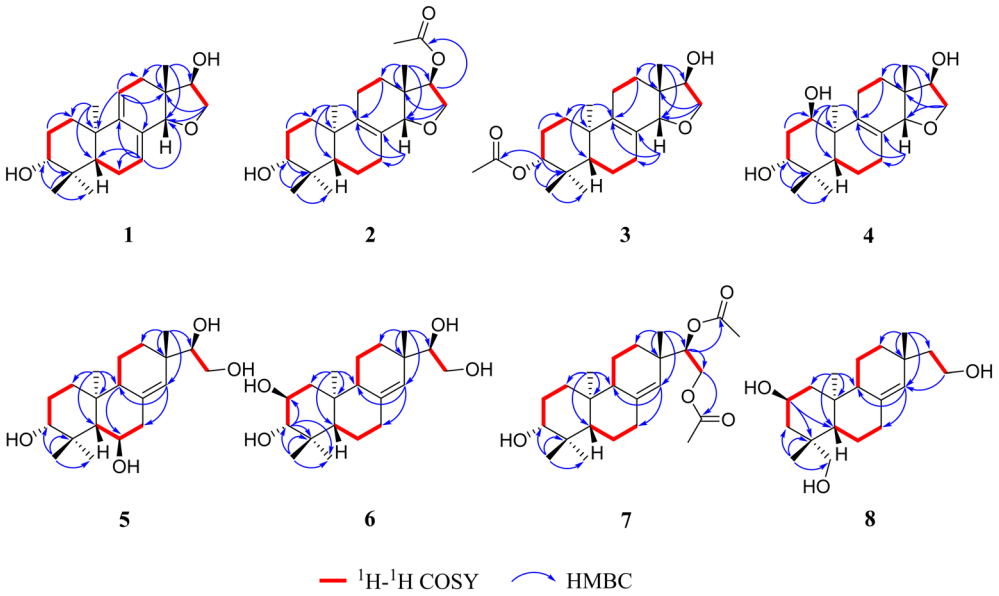

Fig. 2 The key ^{1}H–^{1}H COSY and HMBC (from ^{1}H to ^{13}C) correlations of compounds **1–8**.

s)], an oxygenated methylene protons [δ_H 3.59 (1H, dd, J = 11.9, 1.4 Hz) and 4.30 (1H, dd, J = 11.9, 4.9 Hz)] and four methyl protons [δ_H 0.89 (3H, s), 0.92 (3H, s), 0.98 (6H, s)]. In the ^{13}C NMR and HSQC spectra (Table 1 and Fig. S4), twenty carbon signals were observed, assigned to four methyl, five methylene (including one oxygenated carbon, δ_C 75.3), six methine (including two olefinic carbons, δ_C 115.6 and 131.9 and three oxygenated carbons, δ_C 79.5, 79.6 and 84.7), and five quaternary carbons (including two olefinic carbons, δ_C 129.6 and 144.6). Considering the molecular formula, the degree of unsaturation, and biological source, **1** was considered as an *ent*-pimarene diterpenoid with an oxolane ring group.[20] The ^{1}H–^{1}H COSY correlations of H-15/H$_2$-16 and the HMBC correlations (Fig. S5 and S6) from the protons at δ_H 0.92 (3H, s, H-17) to the carbons at δ_C 34.0 (C-12), δ_C 45.2 (C-13), δ_C 84.7 (C-14), and δ_C 79.5 (C-15) ascertained the location of the oxolane ring between C-14 and C-16. The HMBC correlations from δ_H 5.87 (1H, d, H-7) to δ_C 50.0 (C-5), δ_C 25.0 (C-6), δ_C 144.6 (C-9), δ_C 84.7 (C-14) and from δ_H 5.33 (1H, t, H-11) to δ_C 129.6 (C-8), δ_C 37.6 (C-10), δ_C 34.0 (C-12), and δ_C 45.2 (C-13) confirmed a conjugated diene at $\Delta^{7(8)}$ and $\Delta^{9(11)}$ (Fig. 2 and S5).

Furthermore, the ^{1}H–^{1}H COSY correlations (Fig. S6) of H$_2$-1/H$_2$-2/H-3, H-5/H$_2$-6/H-7 and H-11/H$_2$-12, combined with the correlations from H$_2$-12 to C-9, from H-14 to C-7, C-8, C-9, from H$_3$-18 to C-3, C-4, C-19, and from H$_3$-20 to C-1, C-5, C-10 in the HMBC spectrum (Fig. S5) completed the planar structure of **1**. Therefore, the gross structure of **1** was unambiguously determined to be *ent*-14,16-oxolane-3,15-dihydroxypimar-7,9(10)-

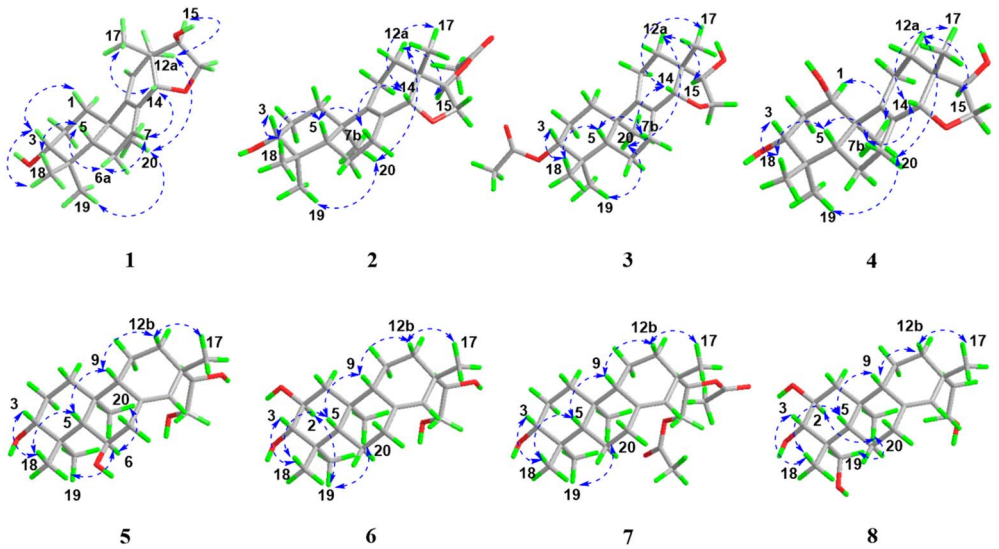

Fig. 3 Energy-minimized conformation with key NOESY correlations for compounds **1–8**.

diene. The NOESY correlations (Fig. S7) of H-3/H_3-18, H-5/H_3-18, H-3/H-5, H-6β/H_3-18, and H-14/H_3-17 indicated that H-3, H-5, H-14, H_3-17, and H_3-18 were located at the β-orientation (Fig. 3). Whereas, the NOESY correlations (Fig. S7) of H_3-19/H_3-20, H_3-20/H-12α, and H-12α/H-15 suggested the α-orientation of H_3-19, H_3-20, and H-15, respectively. Accordingly, the configurations of C-3, C-10, and C-13 were assigned as *R**, *R**, and *R**, respectively. Thus, 3*R*,5*S*,10*R*,13*R*,14*R*,15*R*-**1** (**1a**) and 3*S*,5*R*,10*S*,13*S*,14*S*,15*S*-**1** (**1b**) were proposed to be the model compounds according to the relative configuration established for **1**. Comparing the experimental and theoretical ECD spectra predicted by the time-dependent density functional theory (TDDFT) at the B3LYP/6-311G (d, p) level, the overall pattern of calculated ECD spectrum for **1a** stereoisomer was in good agreement with experimental data of **1** (Fig. 4). Finally, the 3*R*,5*S*,10*R*,13*R*,14*R*,15*R* configuration of **1** was confirmed by X-

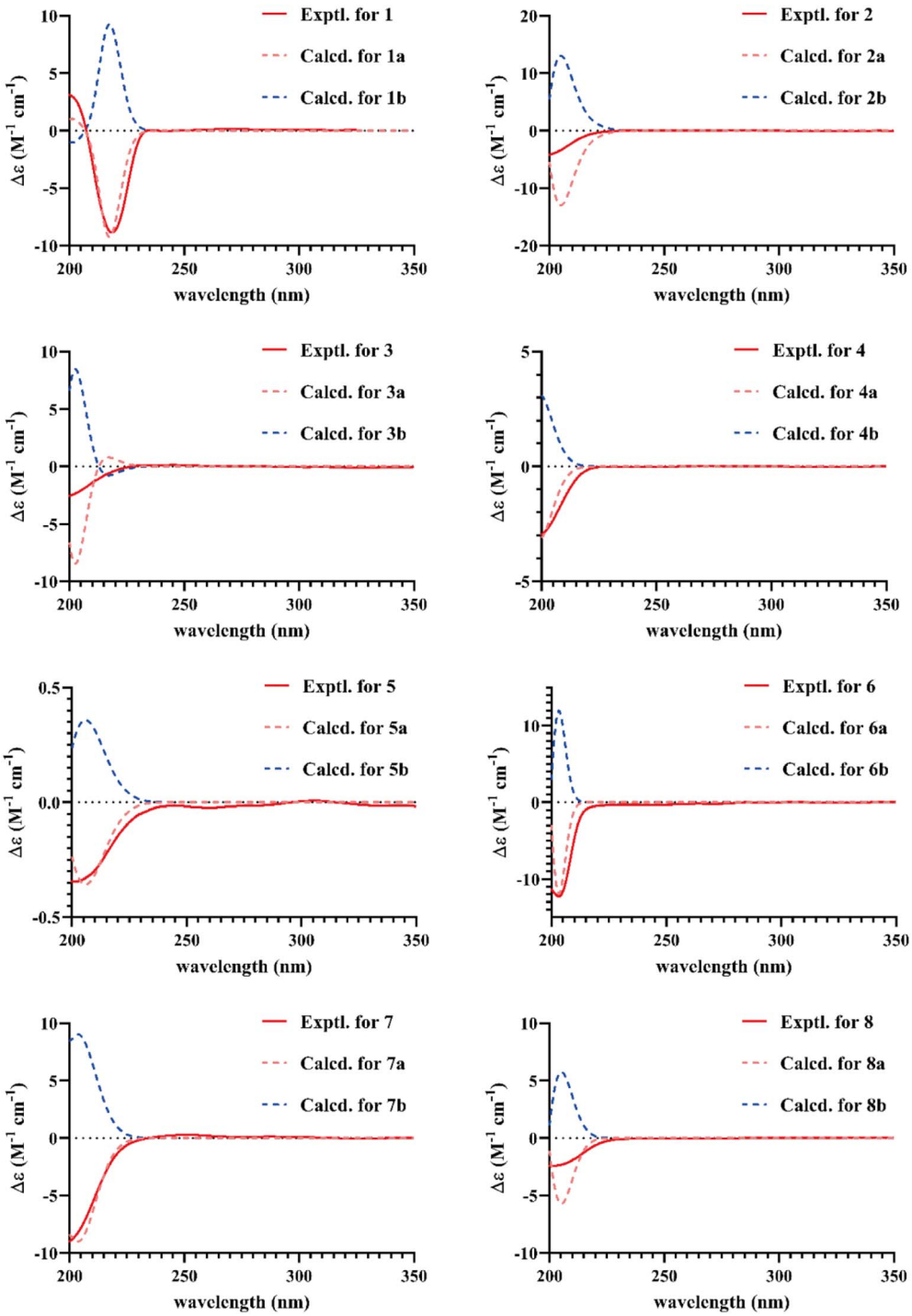

Fig. 4 Calculated or experimental ECD spectra of **1**–**8** in MeOH.

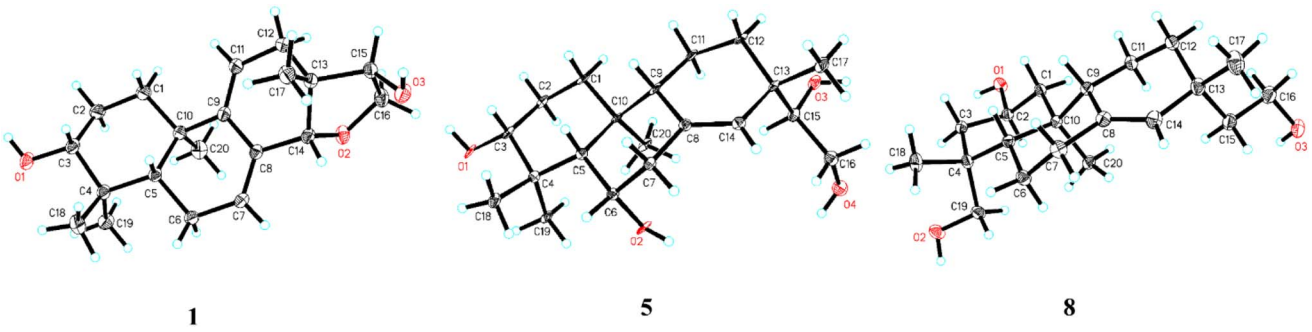

Fig. 5 X-ray ORTEP drawing of compound **1**, **5** and **8**.

ray diffraction analysis of crystals obtained *via* recrystallization from MeOH (Fig. 5). Thus, **1** was established as (3*R*,5*S*,10*R*,13*R*,14*R*,15*R*)-*ent*-14,16-oxolane-3,15-dihydroxypimar-7,9(10)-diene, and it was named as pubescens A.

Compound **2** and compound **3** had the same molecular formula of $C_{22}H_{34}O_4$, as indicated by their ^{13}C NMR data and positive HRESIMS ions at *m*/*z* 385.2349 $[M + Na]^+$ (calcd 385.2349) for **2** and at *m*/*z* 363.2541 $[M + H]^+$ (calcd 363.2530) for **3**. The ^1H and ^{13}C NMR data of these compounds (Tables 1 and 2) were similar to those of *ent*-14β,16-oxolane-8-pimarene-3β,15α-diol[21] except for some differences of substituents. **2** had an acetyl group at C-15, which was supported by the HMBC correlations (Fig. S15) from the protons at δ_H 4.89 (1H, dd, H-15) to the carbons at δ_C 84.5 (C-14), 34.0 (C-12) and the ester carbonyl at δ_C 172.3. Whereas, **3** had an acetyl group at C-3, which was confirmed by the HMBC correlations (Fig. S25) from δ_H 4.48 (1H, dd, H-3) to δ_C 52.0 (C-5), 35.1 (C-1), 28.5 (C-18), and the ester carbonyl at δ_C 172.8. The NOESY correlations (Fig. S17) of H-15/H-12α, H-12α/H_3-20, and H_3-20/H_3-19 revealed the α-orientation of H_3-19, H_3-20, and H-15 of **2**. And the NOESY correlations (Fig. S27) of H-3/H_3-18, H_3-18/H-5, H-5/H-7β, H-7β/H-14, and H-14/H_3-17 indicated the β-orientation of H-3, H-5, H-14, H_3-17, and H_3-18 of **3**. Consequently, the structure of **2** and **3** were elucidated as (3*R*,5*S*,10*R*,13*R*,14*R*,15*R*)-*ent*-15-acetoxy-14,16-oxolane-3-hydroxypimarene-8-ene and (3*R*,5*S*,10*R*,13*R*,14*R*,15*R*)-*ent*-3-acetoxy-14,16-oxolane-15-hydroxypimarene-8-ene, respectively, by comparison of their experimental ECD with calculated data. Compounds **2** and **3** were named as pubescens B and pubescens C (Fig. 4).

Compound **4** was purified as a white powder with a molecular formula of $C_{20}H_{32}O_4$ requiring 5 degrees of unsaturation, which was shown by the $[M + H]^+$ ion at *m*/*z* 337.2389 (calcd for $C_{20}H_{33}O_4$, 337.2373). Its 1D NMR data (Table 2) were similar to those of *ent*-14β,16-oxolane-8-pimarene-3β,15α-diol,[21] except for an extra hydroxymethyl (δ_C 72.5) at C-1. This inference was verified by the COSY cross-peaks of H-1/H_2-2 and the HMBC cross-peaks (Fig. S35 and S36) from δ_H 3.93 (1H, t, H-1) to δ_C 82.3 (C-3), 52.0 (C-5), 141.5 (C-9), and 20.7 (C-20). H-1 appeared as a double doublet with two small coupling constants (2.8 and 2.8 Hz), together with correlations of H-1/H_3-20 in the NOESY spectrum (Fig. S37), indicating the β-orientation of OH-1, C-1 was defined as *R** configured. Finally, according to the comparison of experimental data with calculated ECD data of 1*R*,3*R*,5*S*,10*R*,13*R*,14*R*,15*R*-**4** (**4a**) and 1*S*,3*S*,5*R*,10*S*,13*S*,14*S*,15*S*-**4** (**4b**) (Fig. 4) and biogenetic consideration, **4** was identified as (1*R*,3*R*,5*S*,10*R*,13*R*,14*R*,15*R*)-*ent*-14,16-oxolane-1,3,15-trihydroxypimarene-8-ene, and was named as pubescens D.

Compound **5**, white amorphous powder, gave a $[M + Na]^+$ ion in HRESIMS at *m*/*z* 361.2353 (calcd for 361.2349), consistent with the molecular formula $C_{20}H_{34}O_4$. A comparison of the 1D NMR data of **5** with those of darutigenol (**9**) (Tables 3 and S9) revealed a considerable degree of similarity except for some resonances corresponding to ring B.[22] The large chemical shift difference of C-6 (from δ_C 23.0 in **9** to δ_C 68.7 in **5**) indicated the presence of a OH group in C-6 of **5**, which was confirmed by the COSY cross-peaks of H-5/H-6/H_2-7 and HMBC cross-peaks shown in Fig. 2, S45 and S46. The NOESY cross-peaks of H-6/H_3-19/and H-6/H_3-20, suggested the β-orientation of OH-6 (Fig. 3 and S47). Because of the structure of a *vic*-diol moiety in the side chain, $Mo_2(OAc)_4$ induced ECD was used to suggest the absolute configuration of **5**. According to the rule proposed by Snatzke, the positive Cotton effect at 305 nm in the ECD spectrum of 15*S*,16-dihydroxy-7-oxopimar-8(9)-ene, C-15 was indicated as an *S* configuration.[23,24] On the contrary, the negative sign observed in ECD spectrum of **5** established a 15*R* configuration (Fig. 6).[25,26] Finally, according to the comparison of experimental data with calculated ECD data of 3*R*,5*S*,6*R*,9*R*,10*S*,13*S*,15*R*-**5** (**5a**) and 3*S*,5*R*,6*S*,9*S*,10*R*,13*R*,15*S*-**5** (**5b**) (Fig. 4), the configuration of **5** was defined as 3*R*, 5*S*, 6*R*, 9*R*, 10*S*, 13*S* and 15*R*. And this identification was confirmed by X-ray diffraction analysis of crystals obtained *via* recrystallization from MeOH as shown in Fig. 5. Therefore, the structure of **5** was elucidated as (3*R*,5*S*,6*R*,9*R*,10*S*,13*S*,15*R*)-*ent*-3,6,15,16-tetrahydroxypimar-8(14)-ene and was named as pubescens E.

Compound **6** shared the same molecular formula of $C_{20}H_{34}O_4$ with **5** as determined by the HRESIMS at *m*/*z* 361.2347 $[M + Na]^+$ (calcd for $C_{20}H_{34}NaO_4$, 361.2349). Its 1D NMR spectroscopic data (Table 3) were similar to those of **9**, except for an additional hydroxy group at C-2. Supporting this assignment was the presence of COSY correlation (Fig. S56) of H_2-1/H-2/H-3 and HMBC correlation (Fig. S55) observed from δ_H 2.96 (1H, d, H-3) to δ_C 69.3 (C-2), 40.6 (C-4), 29.6 (C-19), and 16.2 (C-20). The NOESY correlation (Fig. S57) of H-2/H_3-20 suggested that C-2 was *S** configured. Therefore, the structure of **6** was identified as (2*S*,3*S*,5*S*,10*S*,13*S*,15*R*)-*ent*-2,3,15,16-tetrahydroxypimar-

Table 2 ^{1}H and ^{13}C NMR spectroscopic data of compounds **3** and **4** in CD_3OD

	3		**4**	
Position	δ_H (J in Hz)[a]	δ_C[b], type	δ_H (J in Hz)[a]	δ_C[b], type
1a	1.86, dt (13.2, 3.6)	35.1, CH_2	3.93, t (2.8)	72.5, CH
1b	1.25, m			
2a	1.72, m	24.9, CH_2	1.90, td (12.6, 2.8)	35.4, CH_2
2b	1.70, m		1.79, m	
3	4.48, dd (9.6, 7.2)	82.3, CH	3.69, dd (11.9, 4.2)	74.1, CH
4		38.8, C		39.8, C
5	1.22, dd (12.6, 2.4)	52.0, CH	1.62, dd (12.6, 2.1)	44.7, CH
6a	1.77, dd (12.6, 7.2)	19.5, CH_2	1.76, m	19.3, CH_2
6b	1.56, ddd (18.6, 12.6, 6.0)		1.55, ddd (17.5, 12.6, 5.6)	
7a	2.41, td (17.4, 5.4)	31.7, CH_2	2.36, dd (17.5, 4.9)	31.6, CH_2
7b	1.93, m		1.93, m	
8		125.7, C		127.0, C
9		142.7, C		141.5, C
10		38.7, C		43.4, CH
11a	2.05, m	21.9, CH_2	2.32, m	21.3, CH_2
11b	2.03, m		2.08, brd (17.5)	
12a	1.35, m	30.4, CH_2	1.35, dd (12.6, 4.9)	30.5, CH_2
12b	1.33, m		1.27, td (12.6, 4.9)	
13		43.9, C		44.1, C
14	3.56, s	84.1, CH	3.57, s	84.2, CH
15	3.78, dd (5.4, 2.4)	80.5, CH	3.79, dd (5.6, 2.1)	80.6, CH
16a	4.20, dd (9.6, 5.4)	74.6, CH_2	4.20, dd (9.8, 5.6)	74.6, CH_2
16b	3.57, dd (9.6, 5.4)		3.57, dd (9.8, 2.1)	
17	0.93, s	14.6, CH_3	0.96, s	14.8, CH_3
18	0.92, s	28.5, CH_3	1.04, s	28.6, CH_3
19	0.94, s	17.1, CH_3	0.83, s	16.2, CH_3
20	1.05, s	19.7, CH_3	1.01, s	20.7, CH_3
OAc-3	2.04, s	172.8, CH		
		21.1, CH_3		

[a] ^{1}H NMR data (d) were measured in 600 MHz NMR instrument. Proton coupling constants (J) in Hz are given in parentheses. [b] ^{13}C data were recorded at 150 MHz. The assignments were based on ^{1}H–^{1}H COSY, HSQC, HMBC, and NOESY experiments.

8(14)-ene and was named as pubescens F on the basis of the comparison of experimental data with calculated ECD data of 2*S*,3*S*,5*S*,10*S*,13*S*,15*R*-**6** (**6a**) and 2*R*,3*R*,5*R*,10*R*,13*R*,15*S*-**6** (**6b**) (Fig. 4).

Compound **7** was isolated as a white powder. The molecular formula was determined as $C_{24}H_{38}O_5$, based on the HRESIMS ion at m/z 429.2626 $[M + Na]^+$. Its 1D NMR spectroscopic data were similar to those of siegesbeckia Q (**10**) (Tables 4 and S10), except for an extra acetyl group at C-16. This was supported by the 2D NMR experiments (Fig. S64–S67). Thus, the structure of **7** was established as (3*R*,5*S*,9*R*,10*S*,13*S*,15*R*)-*ent*-15,16-diacetoxy-3-hydroxypimar-8(14)-ene and was named as pubescens G according to the comparison of experimental data with calculated ECD data of 3*R*,5*S*,9*R*,10*S*,13*S*,15*R*-**7** (**7a**) and 3*S*,5*R*,9*S*,10*R*,13*R*,15*S*-**7** (**7b**) (Fig. 4).

Compound **8** was assigned a molecular formula of $C_{20}H_{34}O_3$ based on the HRESIMS ion at m/z 323.2596 $[M + H]^+$ (calcd for $C_{20}H_{35}O_3$, 323.2581). The ^{1}H and ^{13}C NMR data of **8** (Table 4) were indicative of the presence of three methyl groups (δ_H 0.82, 0.92 and 1.01), three oxygenated carbons (δ_C 59.9, 65.2 and 65.7). A comparison of the molecular formula and the NMR data of **8** with those of kirenol (**11**) revealed that these two compounds were closely related, with prominent differences being the absence of OH group in C-15 in the side chain. The COSY, HMBC, and NOESY correlations (Fig. S75–S77) matched well with this observation shown in Fig. 2 and 3. According to the comparison of experimental data with calculated ECD data of 2*S*,4*R*,5*S*,9*R*,10*S*,13*R*-**8** (**8a**) and 2*R*,4*S*,5*R*,9*S*,10*R*,13*S*-**8** (**8b**) (Fig. 4), the configuration of **8** was determined as 2*S*, 4*R*, 5*S*, 9*R*, 10*S*, and 13*R*, and was confirmed by single-crystal X-ray diffraction analysis of crystals obtained *via* recrystallization from MeOH (Fig. 5). Therefore, the structure of **8** was identified as (2*S*,4*R*,5*S*,9*R*,10*S*,13*R*)-*ent*-2,16,19-trihydroxypimar-8(14)-ene and was named as pubescens H.

By comparing the spectroscopic data with those reported in the literature, structures of the known compounds were identified as darutigenol (**9**),[22] siegesbeckia Q (**10**),[25] kirenol (**11**),[27] respectively.

Based on our previous study, the 50% ethanol elution of HS inhibited UCHL5/NLRP3 pathway and alleviated myocardial H/R injury, kirenol might be the core active compound.[19] Therefore, compounds **1–10** were tested for the myocardial protective function by H9c2 cell (National Experimental Cell Resource Sharing Platform, Beijing, China) H/R induced myocardial ischemia-reperfusion injury model (kirenol, 10 μM, as a positive control).[19,28] As a result, pubescens H (**8**) showed strong myocardial protective activity in 1 μM. Comparing with the cell viability of 59.80 ± 7.37% in the positive group, the cell viability

Table 3 ^{1}H and ^{13}C NMR spectroscopic data of compounds **5** and **6** in CD_3OD

	5		**6**	
Position	δ_H (J in Hz)[a]	δ_C[b], type	δ_H (J in Hz)[a]	δ_C[b], type
1a	1.66, m	40.8, CH_2	1.96, dd (12.6, 4.2)	46.6, CH
1b	1.21, dd (13.2, 3.6)		1.13, dd (12.6, 2.4)	
2a	1.70, m	28.3, CH_2	3.59, ddd (9.6, 4.2, 2.4)	69.3, CH_2
2b	1.69, m			
3	3.13, dd (11.4, 3.0)	80.1, CH	2.96, d (9.6)	84.2, CH
4		40.9, C		40.6, C
5	1.02, brs	57.3, CH	1.16, dt (12.6, 3.0)	55.6, CH
6a	4.35, brs	68.7, CH	1.62, m	23.4, CH
6b			1.39, ddd (18.6, 12.6, 4.2)	
7a	2.29, brd (14.4)	47.0, CH_2	2.29, ddd (14.4, 4.8, 1.8)	36.9, CH_2
7b	2.25, brd (14.4)		2.06, td (14.4, 5.4)	
8		136.8, C		139.3, C
9	1.72, m	52.1, CH	1.78, t (8.4)	52.2, CH
10		40.0, C		39.9, C
11a	1.60, m	19.1, CH_2	1.59, m	19.5, CH_2
11b	1.58, m		1.56, m	
12a	1.97, m	32.4, CH_2	2.00, dt (12.6, 3.6)	33.2, CH_2
12b	0.97, td (12.0, 4.8)		0.93, td (12.6, 4.8)	
13		38.9, C		38.6, C
14	5.25, s	132.0, CH	5.20, d (1.8)	130.1, CH
15	3.60, brd (9.0)	78.1, CH	3.56, dd (9.0, 2.4)	77.5, CH
16a	3.77, brd (10.2)	64.2, CH_2	3.68, dd (11.4, 2.4)	64.3, CH_2
16b	3.47, brd (10.2)		3.46, dd (11.4, 9.0)	
17	0.87, s	23.2, CH_3	0.84, s	23.0, CH_3
18	1.07, s	28.7, CH_3	0.83, s	17.6, CH_3
19	1.18, s	17.5, CH_3	1.03, s	29.6, CH_3
20	1.10, s	18.5, CH_3	0.87, s	16.2, CH_3

[a] ^{1}H NMR data (d) were measured in 600 MHz NMR instrument. Proton coupling constants (J) in Hz are given in parentheses. [b] ^{13}C data were recorded at 150 MHz. The assignments were based on ^{1}H–^{1}H COSY, HSQC, HMBC, and NOESY experiments.

can be increased to 62.19 ± 12.65%. Pubescens B (**2**) also exhibited good myocardial protective activity in 10 μM, the cell viability can be increased to 37.94 ± 6.28%. Additionally, the known compound darutigenol (**9**) also had great myocardial protective activity in 10 μM (Table 5). Other tested compounds showed no activity in this research. The cytotoxicity of Pubescens B (**2**) and pubescens H (**8**) was also shown in the Fig. S87. According to the data, all tested compounds exhibited no appreciable toxicity in normal H9c2 cell even at a high concentration of 100 μM, but the cell injury was observed when they were applied to cells subjected to hypoxia/reoxygenation (H/R). This result may be caused by the phenomenon that stressed or diseased cells exhibit heightened sensitivity.[29–31]

In order to study the binding mode of active compounds and UCHL5, molecular docking was performed using Autodock 4.2.6. As a result, the binding energy of pubescens B (**2**),

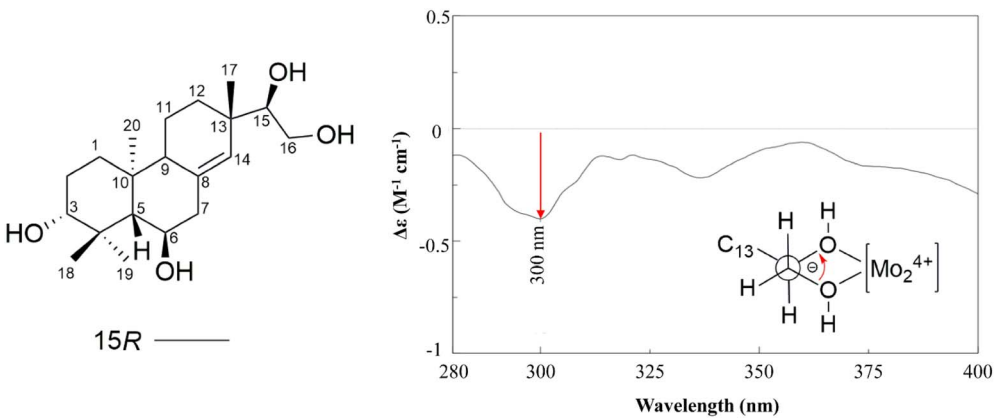

Fig. 6 ECD curves of $Mo_2(OAc)_4$ complex of compound **5**.

Table 4 ^{1}H and ^{13}C NMR spectroscopic data of compounds **7** and **8** in CD_3OD

	7		**8**	
Position	δ_H (J in Hz)[a]	δ_C[b], type	δ_H (J in Hz)[a]	δ_C[b], type
1a	1.70, dt (13.2, 3.0)	38.0, CH_2	2.00, m	49.4, CH_2
1b	1.18, m		1.02, t (12.6)	
2a	1.62, m	28.3, CH_2	3.76, tt (12.6, 4.2)	65.2, CH
2b	1.61, m			
3a	3.20 dd (9.0, 6.6)	79.7, CH	2.17, ddd (12.6,4.2, 2.4)	44.4, CH_2
3b			0.89, td (12.6, 1.2)	
4		40.1, C		41.5, C
5	1.09, dd (12.6, 3.0)	55.6, CH	1.20, dd (12.6, 2.4)	56.5, CH
6a	1.67, m	23.5, CH_2	1.71, m	23.3, CH_2
6b	1.42, dd (12.6, 4.8)		1.30, ddd (18.6, 12.6, 4.2)	
7a	2.32, ddd (14.4, 4.8, 1.8)	37.1, CH_2	2.25, ddd (14.4, 4.2, 1.8)	37.3, CH_2
7b	2.06, m		2.01, m	
8		141.9, C		137.1, C
9	1.73, t (8.4)	51.9, CH	1.79, t (8.4)	52.4, CH
10		39.3, C		40.6, C
11a	1.55, m	19.4, CH_2	1.62, m	20.3, CH_2
11b	1.53, m		1.55, m	
12a	1.70, dt (12.6, 3.6)	33.4, CH_2	1.58, m	36.3, CH_2
12b	1.02, td (12.6, 4.8)		1.15, td (12.6, 4.8)	
13		38.3, C		33.9, C
14	5.19, brs	127.4, CH	5.23, brs	132.5, CH
15a	5.16, dd (9.0, 2.4)	75.9, CH	1.63, m	45.1, CH_2
15b			1.53, m	
16a	4.44, dd (12.0, 2.4)	64.8, CH_2	3.63 td (10.2, 6.0)	59.9, CH_2
16b	4.06, dd (12.0, 9.0)		3.57, td (10.2, 6.0)	
17	0.97, s	23.5, CH_3	0.92, s	28.9, CH_3
18	1.00, s	29.1, CH_3	1.01, s	28.0, CH_3
19a	0.82, s	16.5, CH_3	3.68, d (10.8)	65.7, CH_2
19b			3.33, d (10.8)	
20	0.85, s	16.1, CH_3	0.82, s	17.3, CH_3
OAc-15	2.06, s	172.5, C		
		20.8, CH_3		
OAc-16	1.98, s	172.5, C		
		20.7, CH_3		

[a] ^{1}H NMR data (d) were measured in 600 MHz NMR instrument. Proton coupling constants (J) in Hz are given in parentheses. [b] ^{13}C data were recorded at 150 MHz. The assignments were based on ^{1}H–^{1}H COSY, HSQC, HMBC, and NOESY experiments.

pubescens H (**8**), darutigenol (**9**) and kirenol (**11**) were −7.5, −6.1, −6.3 and −6.3 kJ mol^{-1}, respectively. As shown in Fig. 7A, pubescens B (**2**) had a good interaction with UCHL5 through hydrophobic interactions with residues [Leu-38, Glu-205, Ile-208, Ser-37, Ile-35, Phe 218 and Trp-36]. As shown in Fig. 7B, pubescens H (**8**) formed three hydrogen bonds with the interacting residues Glu-113, Ala-129 and Asn-132. Ala-129 and Asn-132 were involved in hydrogen bonding interactions with the hydroxyl group at C-16. Pubescens H (**8**) also had hydrophobic interactions with residues [Val-135, Ser-133, Phe-114 and Phe-117]. As shown in Fig. 7C, darutigenol formed two hydrogen bonds with the interacting residues Trp-36 and Ile-35. Trp-36 and Ile-35 were involved in hydrogen bonding interactions with the hydroxyl group at C-16. Darutigenol had hydrophobic interactions with residues [Gln-209, Ser-37, Phe-218, Ile-208, Glu-39 and Glu-205]. As shown in Fig. 7D, kirenol formed four hydrogen bonds with the interacting residues Glu-113, Ala-129 and Asn-132. Asn-132 were involved in hydrogen bonding

Table 5 The activity of compounds on H9c2 cells[a]

		Cell viability (%)				
Compound	Control	H/R	Kirenol 10 μM	1 μM	10 μM	50 μM
2	100.00 ± 5.15	20.69 ± 4.36*	46.39 ± 7.58$^{\#}$	29.37 ± 2.19	37.94 ± 6.28$^{\#}$	26.92 ± 0.77
8	98.80 ± 2.95	37.90 ± 4.19*	59.80 ± 7.37$^{\#}$	62.19 ± 12.65$^{\#}$	57.42 ± 9.39$^{\#}$	51.46 ± 9.83$^{\#}$
9	103.77 ± 4.65	53.02 ± 7.07*	61.76 ± 6.83$^{\#}$	63.18 ± 7.21	76.21 ± 6.22$^{\#}$	66.18 ± 20.37$^{\#}$

[a] $n = 6$, *$P < 0.05$ *vs.* Sham, $^{\#}P < 0.05$ *vs.* H/R, and the time of treatment: 24 h.

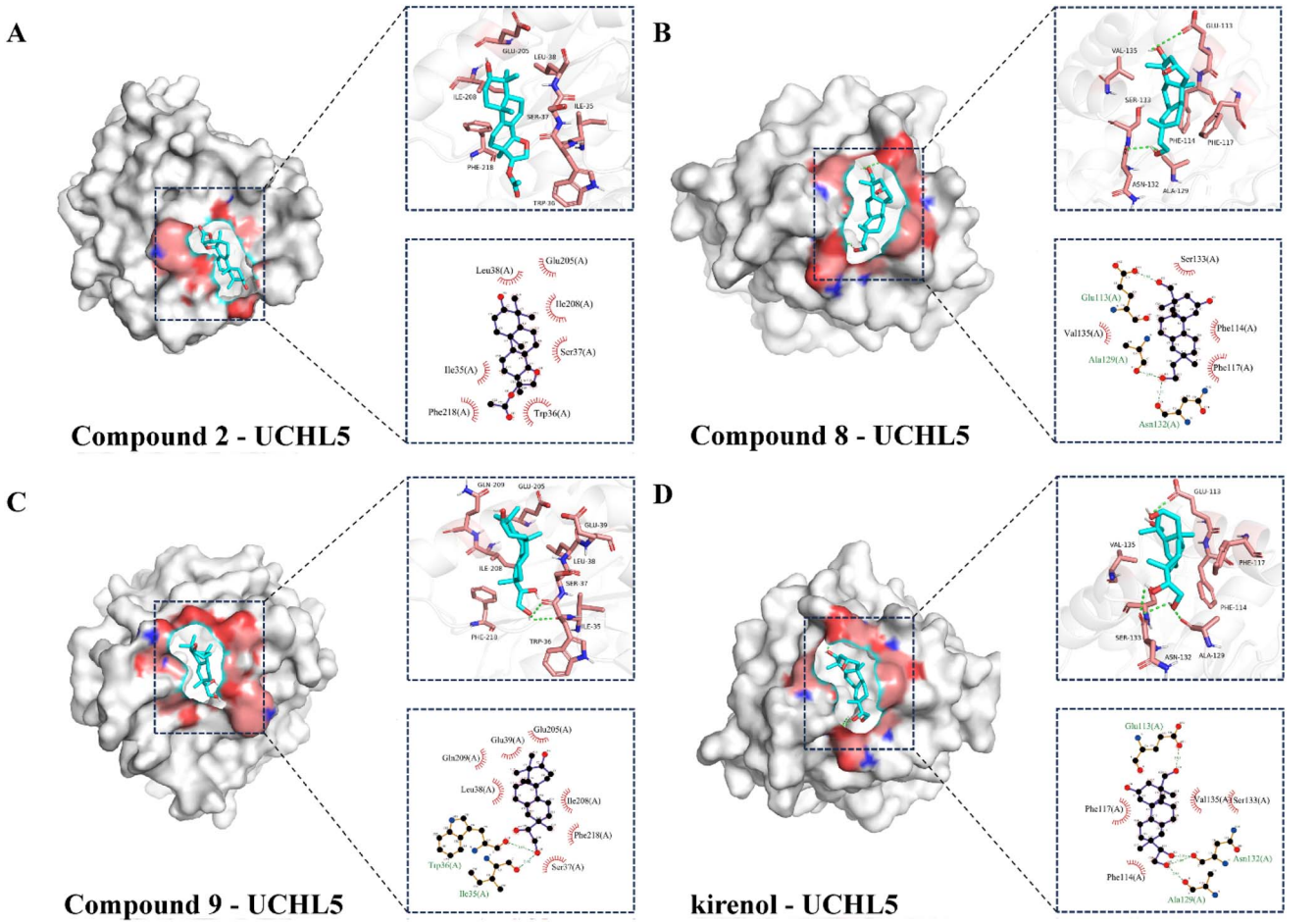

Fig. 7 Molecular docking of compound 2, 8, 9 and kirenol with UCHL5.

interactions with the hydroxyl group at C-15 and C-16. Kirenol also had hydrophobic interactions with residues [Val-135, Ser-133, Phe-114 and Phe-117].

Conclusions

Phytochemical investigation of EtOAc extract of the bark of the dried aerial parts of *S.pubescens* yielded the isolation and identification of eight previously undescribed diterpenoids, named pubescens A–H (**1–8**), and 3 known compounds. The absolute configuration of pubescens A (**1**), pubescens E (**5**) and pubescens H (**8**) were established by single-crystal X-ray diffraction. Additionally, these compounds were tested for the myocardial protective function by H9c2 cell H/R induced myocardial ischemia-reperfusion injury model. In conjunction with the molecular docking with UCHL5, new compounds pubescens B (**2**) and pubescens H (**8**) displayed good myocardial protective activity similar to the typical active compound kirenol (**11**). Pubescens B and pubescens H could be selected for further study. In conclusion, this study enriched the chemical composition of *S. pubescens*, preliminarily screened the myocardial protective activity of compounds, explored the binding mode between active compounds and UCHL5 and also provided a basis for further study.

Experimental section

General experimental procedures

Optical rotations were measured on a Rudolph Research Autopol III automatic polarimeter. UV spectra were measured on a Cary 300 spectrometer. ECD spectra were recorded on a JASCO J-815 spectrometer. IR spectra were obtained on a Nicolet Impact 400 FT-IR Spectrophotometer. 1D and 2D NMR spectra were recorded on a Bruker ARX-600 spectrometer with solvent peaks as references. HRESIMS data were obtained with an Agilent 1290 Infinity liquid chromatography system and an Agilent 6546 QTOF mass spectrometer. High-performance liquid chromatography (HPLC) data were recorded on a SHIMADZU LC-20AT equipped with a CBM-20A, an SPD-M20A and a MGII C_{18} column (250 × 4.6 nm, 5 μm). Preparative HPLC was performed on SHIMADZU LC-16P with an SPD-16, a RID-20A and a MGII C_{18} column (250 × 20 nm, 5 μm). Column chromatographic separations were carried out with silica gel (100–200 and 200–300 mesh, Qingdao Marine Chemical Group Corporation, Qingdao, China), MCI gel (CHP20/P120, MITSUBUSHI Chemical Corporation, Japan), Sephadex LH-20 (17-0090-02, GE Healthcare, Sweden) and ODS (Grace, USA). TLC was conducted with glass precoated with silica gel GF254

(Qingdao Marine Chemical Group Corporation, Qingdao, China). All solvents were purchased from Innochem.

Plant material

S. pubescens was purchased from Dongzhimen Hospital, Beijing University of Chinese Medicine and produced by Beijing Sanhe Pharmaceutical Limited Company. The plant material was identified by Researcher Zhan Zhilai at Chinese Medicine Resource Center, Institute of Traditional Chinese Medicine, Chinese Academy of Chinese Medical Sciences.

Extraction and isolation

The dried aerial parts of *S. pubescens* (15 kg) were extracted under reflux with 95% EtOH three times. The solvent was evaporated under reduced pressure to yield the aqueous residue, which was then extracted with EtOAc, the EtOAc extract (500 g) was subjected to silica gel column chromatography (CC) and eluted with petroleum ether–acetone (100 : 0 to 0 : 100) to yield 13 fractions (Fr.1–Fr.13).

Fr.6 and Fr.7 (66.7 g) were combined and subjected to silica gel column chromatography (CH_2Cl_2–MeOH, 100 : 0 to 0 : 100) to afford subfractions Fr.6.1, Fr.6.2, Fr.6.3, Fr.6.4 and Fr.6.5. Subsequently, Fr.6.1 was subjected to Sephadex LH-20 CC (5 × 120 cm) eluting with MeOH and further separated by preparative HPLC [ACE-C_{18}, 5 μm, 250 × 10 mm, ACN–H_2O–TFA (90 : 10 : 0.1)] to afford compound **9** (3.8 mg, t_R 5.5 min). Fr.6.2 was subjected to Middle Chromatogram Isolated Gel (MCI) eluting with MeOH–H_2O (90 : 10 to 100 : 0) and further separated by preparative HPLC [CN-C_{18}, 5 μm, 250 × 10 mm, ACN–H_2O–TFA (30 : 70 : 0.1)] to afford compounds **2** (3.3 mg, t_R 28.0 min), **3** (1.0 mg, t_R 26.5 min), **7** (1.5 mg, t_R 32.5 min) and **10** (2.0 mg, t_R 18.0 min).

Fr.8 and Fr.9 were combined and performed on reversed phase medium pressure CC with MeOH–H_2O (5 : 95 to 100 : 0), yielding 8 subfractions Fr.8.1–Fr.8.8. Separation on Fr.8.6 by Sephadex LH-20 CC (5 × 120 cm) eluting with MeOH afforded 6 subfractions Fr.8.6.1–Fr.8.6.6. Fr.8.6.2 was further separated by preparative HPLC [UG-C_{18}, 5 μm, 250 × 10 mm, ACN–H_2O (39 : 61)] to afford compounds **1** (2.9 mg, t_R 31.0 min) and **4** (2.2 mg, t_R 27.0 min). Fr.8.7 was subjected to Sephadex LH-20 CC (5 × 120 cm) eluting with CH_2Cl_2–MeOH (50 : 50) and silica gel column chromatography (CH_2Cl_2–MeOH, 100 : 0 to 10 : 90) to afford 12 subfractions Fr.8.7.1–Fr.8.7.12. Fr.8.7.4 was further separated by preparative HPLC [MGII-C_{18}, 5 μm, 250 × 10 mm, ACN–H_2O (30 : 70)] to afford compounds **5** (1.9 mg, t_R 36.0 min), **6** (1.5 mg, t_R 34.5 min) and **8** (2.3 mg, t_R 39.0 min). Fr.8.7.11 was further separated by preparative HPLC [SP-C_{18}, 5 μm, 250 × 10 mm, ACN–H_2O (42 : 58)] to afford compound **11** (10.5 mg, t_R 32.5 min).

Pubescens A (1). White powder; [α] +52.0 (*c* 0.01, MeOH); UV (MeOH, 0.001) λ_{max} (log ε) 204 (4.23), 231 (2.28), 284 (0.30) nm; FT-IR (ATR) ν_{max} 3387, 2932, 1682, 1456, 1375, 1208, 1140, 1094, 1038, 1004, 967, 917, 843, 802, 724, 666 cm^{-1}; ^1H NMR (700 MHz, CD_3OD) and ^{13}C NMR (150 MHz, CD_3OD) data, see Tables 1 and 2; HRESIMS *m*/*z* 319.2276 $[M + H]^+$ (calcd for $C_{20}H_{31}O_3$, 319.2267).

Pubescens B (2). White powder; [α] +1.0 (*c* 0.01, MeOH); UV (MeOH, 0.001) λ_{max} (log ε) 205 (0.31), 247 (0.07) nm; FT-IR (ATR) ν_{max} 3445, 2925, 2871, 1740, 1687, 1456, 1374, 1246, 1208, 1187, 1093, 1033, 979, 933, 843, 803, 725, 649, 607 cm^{-1}; ^1H NMR (600 MHz, CD_3OD) and ^{13}C NMR (150 MHz, CD_3OD) data, see Tables 1 and 2; HRESIMS *m*/*z* 385.2349 $[M + H]^+$ (calcd for $C_{22}H_{34}NaO_4$, 385.2349).

Pubescens C (3). White powder; [α] +1.0 (*c* 0.01, MeOH); UV (MeOH, 0.001) λ_{max} (log ε) 204 (0.32), 242 (0.10) nm; FT-IR (ATR) ν_{max} 3445, 2940, 2873, 1734, 1704, 1682, 1644, 1453, 1374, 1246, 1207, 1185, 1138, 1032, 978, 842, 802, 724 cm^{-1}; ^1H NMR (600 MHz, CD_3OD) and ^{13}C NMR (150 MHz, CD_3OD) data, see Tables 1 and 2; HRESIMS *m*/*z* 363.2541 $[M + H]^+$ (calcd for $C_{22}H_{35}O_4$, 363.2530).

Pubescens D (4). White powder; [α] −8.0 (*c* 0.01, MeOH); UV (MeOH, 0.001) λ_{max} (log ε) 204 (0.28), 283 (0.02) nm; FT-IR (ATR) ν_{max} 3386, 2926, 2881, 1680, 1446, 1377, 1260, 1206, 1140, 1090, 1037, 1005, 917, 842, 801, 660, 628 cm^{-1}; ^1H NMR (700 MHz, CD_3OD) and ^{13}C NMR (150 MHz, CD_3OD) data, see Tables 1 and 2; HRESIMS *m*/*z* 337.2389 $[M + H]^+$ (calcd for $C_{20}H_{33}O_4$, 337.2373).

Pubescens E (5). White powder; [α] +16.0 (*c* 0.01, MeOH); UV (MeOH, 0.001) λ_{max} (log ε) 204 (0.26), 281 (0.02) nm; FT-IR (ATR) ν_{max} 3381, 2930, 2852, 1682, 1446, 1379, 1208, 1140, 1054, 1015, 844, 802, 725, 683, 655, 623, 607 cm^{-1}; ^1H NMR (600 MHz, CD_3OD) and ^{13}C NMR (150 MHz, CD_3OD) data, see Tables 1 and 2; HRESIMS *m*/*z* 361.2353 $[M + Na]^+$ (calcd for $C_{20}H_{34}NaO_4$, 361.2349).

Pubescens F (6). White powder; [α] −7.0 (*c* 0.01, MeOH); UV (MeOH, 0.001) λ_{max} (log ε) 205 (0.20); FT-IR (ATR) ν_{max} 3388, 2940, 2875, 1679, 1455, 1434, 1261, 1203, 1140, 1055, 1032, 996, 802, 722, 655, 621 cm^{-1}; ^1H NMR (600 MHz, CD_3OD) and ^{13}C NMR (150 MHz, CD_3OD) data, see Tables 1 and 2; HRESIMS *m*/*z* 361.2347 $[M + Na]^+$ (calcd for $C_{20}H_{34}NaO_4$, 361.2349).

Pubescens G (7). White powder; [α] −18.0 (*c* 0.01, MeOH); UV (MeOH, 0.001) λ_{max} (log ε) 205 (0.63), 240 (0.17) nm; FT-IR (ATR) ν_{max} 3445, 2940, 2867, 1743, 1698, 1647, 1456, 1434, 1371, 1244, 1227, 1142, 1093, 1033, 968, 942, 866, 835, 803, 724, 617, 607 cm^{-1}; ^1H NMR (600 MHz, CD_3OD) and ^{13}C NMR (150 MHz, CD_3OD) data, see Tables 1 and 2; HRESIMS *m*/*z* 429.2626 $[M + Na]^+$ (calcd for $C_{24}H_{38}NaO_5$, 429.2611).

Pubescens H (8). White powder; [α] −27.0 (*c* 0.01, MeOH); UV (MeOH, 0.001) λ_{max} (log ε) 205 (0.37), 281 (0.01) nm; FT-IR (ATR) ν_{max} 3334, 2937, 2871, 2831, 1681, 1455, 1363, 1206, 1143, 1032, 996, 965, 655 cm^{-1}; ^1H NMR (600 MHz, CD_3OD) and ^{13}C NMR (150 MHz, CD_3OD) data, see Tables 1 and 2; HRESIMS *m*/*z* 323.2596 $[M + H]^+$ (calcd for $C_{20}H_{35}O_3$, 323.2581).

X-ray crystal structure analysis of compounds 1, 5 and 8

Crystallographic data for the structures of **1**, **5** and **8** have been deposited with the Cambridge Crystallographic Data Centre (CCDC 2453116 for **1**; CCDC 2453118 for **5**; CCDC 2453134 for **8**).

X-ray crystallographic data for 1. $C_{20}H_{32}O_4$ (M = 336.45): monoclinic, space group $P2_1$ (no. 4); a = 6.84365 (12) Å, b = 11.17471 (20) Å, c = 11.9856 (2) Å, β = 92.9687 (16)°, V = 915.38

(3) Å^3, $Z = 2$, $T = 169.99$ (10) K, μ (Cu Kα) = 0.663 mm^{-1}, D_{calc} = 1.221 g cm^{-3}, 6787 reflections measured (7.386° ≤ 2Θ ≤ 148.144°), 3579 unique (R_{int} = 0.0210, R_{sigma} = 0.0247) which were used in all calculations. The final R_1 was 0.0299 ($I > 2\sigma(I)$) and wR_2 was 0.0843 (all data).

X-ray crystallographic data for 5. $C_{20}H_{34}O_4$ (M = 338.47): orthorhombic, space group $P2_12_12_1$ (no. 19); a = 7.3800 (4) Å, b = 12.1066 (4) Å, c = 20.3919 (10) Å, V = 1821.95 (15) Å^3, $Z = 4$, T = 149.99 (10) K, μ (Cu Kα) = 0.667 mm^{-1}, D_{calc} = 1.234 g cm^{-3}, 20 517 reflections measured (8.494° ≤ 2Θ ≤ 148.322°), 3654 unique (R_{int} = 0.1125, R_{sigma} = 0.0672) which were used in all calculations. The final R_1 was 0.0765 ($I > 2\sigma(I)$) and wR_2 was 0.2114 (all data).

X-ray crystallographic data for 8. $C_{20}H_{34}O_3$ (M = 322.47): monoclinic, space group $P2_1$ (no. 4), a = 11.2450 (3) Å, b = 7.2402 (2) Å, c = 11.5790 (3) Å, β = 99.615 (3)°, V = 929.48 (5) Å^3, $Z = 2$, T = 170.00 (10) K, μ (Cu Kα) = 0.588 mm^{-1}, D_{calc} = 1.152 g cm^{-3}, 7872 reflections measured (7.744° ≤ 2Θ ≤ 147.56°), 3472 unique (R_{int} = 0.0258, R_{sigma} = 0.0273) which were used in all calculations. The final R_1 was 0.0338 ($I > 2\sigma(I)$) and wR_2 was 0.0859 (all data).

Methodology for ECD analysis

All calculations were performed using Gaussian 16.1. Conformation search using molecular mechanics calculations was performed in DS (Discovery Studio) 2018 with MMFF94 s force field with 20 kcal mol^{-1} upper energy limit at best level. The conformers performed with the DS 2018 software package were further optimized by using the TDDFT method at the B3LYP/6-31G(d, p) level, and the frequency was calculated at the same level of theory. For all optimized structures, vibrational spectra were calculated to ensure that no imaginary frequencies for energy minimum were obtained. The average values were obtained by the Boltzmann distributions, using the relative Gibbs free energies as weighting factors. The stable conformers were subjected to ECD calculation by the TDDFT method at the B3LYP/6-311G+(d,p) level with the CPCM model in MeOH. ECD spectra of different conformers were simulated using SpecDis 1.71 with a half-bandwidth of 0.3 eV, and the final calculated ECD spectra were obtained according to the Boltzmann-calculated contribution of each con-former. The calculated ECD spectra were compared with the experimental data. Additional details are provided in SI (pages 86–117).

Bioactivity assay

H9c2 cardiomyocytes (National Experimental Cell Resource Sharing Platform, Beijing, China) were cultured with glucose-free, fetal bovine serum-free DMEM and incubated in 1% O_2 and 5% CO_2 mixed with 94% N_2 for 6 h, followed by re-oxygenation for 18 h to establish the H/R model. The cells were divided into blank group, model group, positive group, low-dose group, medium-dose group and high-dose experimental group. Except for the blank group, the remaining groups established the H/R injury model. The positive group was supplemented with kirenol at 10 μM. The test for each compound was conducted individually. The experimental groups were supplemented with tested compounds at 1, 10 and 50 μM, respectively. The blank group and model group received the same volume of serum-free and glucose-free. All data were expressed as the mean ± SD values. All data were analyzed by GraphPad Prism 8.0 software and compared using one-way analysis of variance. Statistical significance was considered when the probability was <0.05.

Molecular docking

Protein and ligand preparation. The three-dimensional structure of the target protein was retrieved from the Protein Data Bank (RCSB) (https://www.rcsb.org/), and download the PDB format file. In Pymol 2.5, removed redundant ligands, then configured the protein in AutoDock as follows: remove water, replace with hydrogen, designate the protein as the receptor, and save the structure as a PDBQT protein receptor file. The drug molecular structures were download from the PubChem database (https://pubchem.ncbi.nlm.nih.gov/). Converted the SDF format to PDB format using the OpenBabel GUI software. Similarly, in AutoDock, we configured the drug as follows: remove water, add hydrogen, and set the drug as a ligand. The software automatically configured the torsion tree. We exported the ligand file in PDBQT format.

Grid box dimensions and parameters. The PDBQT structures of the receptor and ligand were imported into AutoDock to define the molecular docking range. With the target protein as the grid center, adjusted the center coordinates (center −23.9/2.075/−8.161) and box size (size 110/54/92) parameters to ensure complete coverage of the protein within the docking box.

Docking protocol and scoring function. In AutoDock Vina, molecular docking was performed by detecting protein macromolecules and inserting small drug molecules, as well as configuring operational methods and docking parameters. The PDBQT format was used to calculate the minimum binding energy. The PyMol 2.5 software converted the combined PDBQT format into PDB format. Finally, for visualization, PyMol 2.5 and Ligplot v.2.29 were used to process the composite PDB format file.

Author contributions

Wanting Li: writing – original draft, methodology, investigation, formal analysis, data curation. Guiyang Xia: writing – review and editing, validation, software, formal analysis, data curation. Jinyu Xia: formal analysis, methodology, investigation. Qiyao Liu: investigation, formal analysis, data curation. Xue-Fen Wu: investigation, data curation. Linnan Zhou: investigation, data curation. Xiaohong Wei: methodology, data curation. Huan Xia: writing – review and editing, methodology, investigation, formal analysis, data curation. Sheng Lin: supervision, project administration, funding acquisition, conceptualization.

Conflicts of interest

The authors declare no conflict of interest.

Data availability

The data supporting this article have been included as part of the supplementary information (SI). Supplementary information: HRESIMS, IR, UV, CD and NMR spectra for compounds **1–8**. NMR spectra for compounds **9–11**. X-ray crystallographic data for compounds **1**, **5** and **8**. ECD details for compounds **1–8**. The cytotoxicity data for **2** and **8**. The FCF data for compounds **1**, **5** and **8**. See DOI: https://doi.org/10.1039/d5ra09664b.

CCDC 2453116, 2453118 and 2453134 contain the supplementary crystallographic data for this paper.[32a–c]

Acknowledgements

This work was financially supported by the National Natural Science Foundation of China (82574555 and 82430116); the Special Fund of Central Committee High Level Chinese Medicine Hospital (CZ015-DZMG-LJRC-0014 and CZ015-DZMG-ZJXY-23013) and the Fundamental Research Funds for the Central Universities (2024-JYB-058).

References

1 Q. Wang, Y. Y. Liang, K. W. Li, Y. Li, F. J. Niu, S. J. Zhou, H. C. Wei and C. Z. Zhou, *J. Ethnopharmacol.*, 2021, **275**, 114117, DOI: 10.1016/j.jep.2021.114117.

2 Chinese Pharmacopoeia Commission, *Pharmacopoeia of the People's Republic of China*, China Medical Science, 2020, vol. 1.

3 Z. Xia, Y. Yin, C. Xia, Y. Zhang, W. Zhang, D. Chen, H. Zhao and Y. Huang, *Chin. J. Geriatr. Heart, Brain Vessel Dis.*, 2018, **20**, 1016–1018.

4 H. Guo, Y. Zhang, B. Cheng, X. Fu, P. Zhu, J. Chen, Y. Chan, C. Yin, Y. Wang, M. Hossen, A. Amin, A. Tse and Z. Yu, *BioSci. Trends*, 2018, **12**, 330–337, DOI: 10.5582/bst.2018.01103.

5 C. Chen, Z. L. Feng, J. Petrović, M. Soković, Y. Ye and L. G. Lin, *Acta Mater. Med.*, 2023, **2**, 357–376, DOI: 10.15212/AMM-2023-0026.

6 X. H. Liu, D. U. Yajun, G. X. Liu, G. M. Dan, X. Tong and J. Xiao, *J. South. Med. Univ.*, 2019, **39**, 1387–1392.

7 B. Xiao, J. Li, Z. Qiao, S. Yang, H. Kwan, T. Jiang, M. Zhang, Q. Xia, Z. Liu and T. Su, *J. Ethnopharmacol.*, 2023, **5**, 116852, DOI: 10.1016/j.jep.2023.116852.

8 B. Wu, X. Y. Huang, L. Li, X. H. Fan, P. C. Li, C. Q. Huang, J. Xiao, R. Gui and S. Wang, *J. Cell. Mol. Med.*, 2019, **23**, 7651–7663, DOI: 10.1111/jcmm.14638.

9 J. Liu, Z. Ge, X. Jiang, J. Zhang, J. Sun and X. Mao, *Chin. J. Nat. Med.*, 2023, **21**, 499–515, DOI: 10.1016/S1875-5364(23)60410-8.

10 P. Yanpiset, C. Maneechote, S. Sriwichaiin, N. Siri-Angkul, S. C. Chattipakorn and N. Chattipakorn, *Acta Pharm. Sin. B*, 2023, **13**, 29–53, DOI: 10.1016/j.apsb.2022.08.007.

11 C. Zhang, S. J. Cai, W. Y. Cheng, N. M. Deng, Y. H. Han and C. Chen, *J. South. Agric.*, 2014, **45**, 1060–1064.

12 D. Wang, X. Dong, Y. Nie, W. Yang and C. Li, *Rec. Nat. Prod.*, 2022, **6**, 515–537, DOI: 10.25135/rnp.317.2201.2332.

13 T. Xue, R. Liu, H. Chen, M. E. Hussien Ibrahim, J. Dong, W. Zhao, L. Chen, H. Fu and J. Wang, *Nat. Prod. Res.*, 2024, 1–15, DOI: 10.1080/14786419.2024.2426203.

14 M. Liu, T. Luo, R. Li, W. Yin, F. Yang, D. Ge and N. Liu, *Chin. J. Nat. Med.*, 2025, **23**, 234–244, DOI: 10.1016/S1875-5364(25)60827-2.

15 Y. Chen, R. Tian, J. Xue, J. Yu and H. Wang, *MedComm: Future Med.*, 2022, **1**, e21, DOI: 10.1002/mef2.21.

16 C. Zhang, X. Chang, D. Zhao, Y. He, G. Dong and L. Gao, *J. Pharm. Anal.*, 2024, **15**, 101051, DOI: 10.1016/j.jpha.2024.101051.

17 X. Wei, Q. Wang, W. Wen, L. Yang, H. Chen, G. Xu, Y. Zhou, J. Yang and Z. Duan, *MedComm: Future Med.*, 2025, **4**, e70016, DOI: 10.1002/mef2.70016.

18 X. Wei, Y. Wu, H. Pan, Q. Zhang, K. He, G. Xia, H. Xia, S. Lin and H. Shang, *Front. Cardiovasc. Med.*, 2022, **6**, 895797, DOI: 10.3389/fcvm.2022.895797.

19 X. Wu, H. Xia, W. Li, J. Chen, L. Zhou, Q. Zhang, H. Shang, G. Xia, X. Wei and S. Lin, *Acta Mater. Med.*, 2024, **3**, 365–382, DOI: 10.15212/AMM-2024-0030.

20 Y. Xiang, H. Zhang, C. Q. Fan and J. M. Yue, *J. Nat. Prod.*, 2004, **67**, 1517–1521, DOI: 10.1021/np0400407.

21 F. Wang, X. Cheng, Y. Li, S. Shi and J. Liu, *J. Nat. Prod.*, 2009, **72**, 2005–2008, DOI: 10.1021/np900449r.

22 J. Wang, H. Duan, Y. Wang, B. Pan, C. Gao, C. Gai, Q. Wu and H. Fu, *J. Nat. Prod.*, 2017, **80**, 19–29, DOI: 10.1021/acs.jnatprod.6b00150.

23 M. Politi, N. De Tommasi, G. Pescitelli, L. Di Bari, I. Morelli and A. Braca, *J. Nat. Prod.*, 2002, **65**, 1742–1745, DOI: 10.1021/np020260p.

24 M. Górecki, E. Jabłońska, A. Kruszewska, A. Suszczyńska, Z. Urbańczyk-Lipkowska, M. Gerards, J. W. Morzycki, W. J. Szczepek and J. Frelek, *J. Org. Chem.*, 2007, **72**, 2906–2916, DOI: 10.1021/jo062445x.

25 Y. Zheng, Z. Guo, H. Chen, T. Bao, X. Gao, A. Wang and J. Jia, *Phytochemistry*, 2023, **205**, 113503, DOI: 10.1016/j.phytochem.2022.113503.

26 K. Fan, L. Zhang, B. Tan, G. S. S. Njateng, M. Qin, R. Guo, X. Huang, C. F. Ding, W. Gao, R. Zhang and H. Yu, *Chin. J. Nat. Med.*, 2023, **21**, 146–153, DOI: 10.1016/S1875-5364(23)60393-0.

27 K. Liu and E. Röder, *Planta Med.*, 1991, **57**, 395–396, DOI: 10.1055/s-2006-960129.

28 J. Y. Jia, E. H. Zang, L. J. Lv, Q. Y. Li, C. H. Zhang, Y. Xia, L. Zhang, L. S. Dang and M. H. Li, *Chin. Herb. Med.*, 2020, **13**, 49–63, DOI: 10.1016/j.chmed.2020.09.002.

29 E. Murphy and C. Steenbergen, *Physiol. Rev.*, 2008, **88**, 581–609, DOI: 10.1152/physrev.00024.2007.

30 A. B. Lentsch, A. Kato, H. Yoshidome, K. M. McMasters and M. J. Edwards, *Hepatology*, 2000, **32**, 169–173, DOI: 10.1053/jhep.2000.9323.

31 J. V. Bonventre and L. Yang, *J. Clin. Invest.*, 2011, **121**, 4210–4221, DOI: 10.1172/JCI45161.

32 (*a*) CCDC 2453116: Experimental Crystal Structure Determination, 2026, DOI: 10.5517/ccdc.csd.cc2nbnsg; (*b*) CCDC 2453118: Experimental Crystal Structure Determination, 2026, DOI: 10.5517/ccdc.csd.cc2nbnvj; (*c*) CCDC 2453134: Experimental Crystal Structure Determination, 2026, DOI: 10.5517/ccdc.csd.cc2nbpc2.